Steric Factors on Unsymmetrical *O*-hydroxyaryl *N*-Heterocyclic Carbene Ligands Prevailing the Stabilization of Single Stereoisomer of Bis-Ligated Titanium Complexes

*Coralie C. Quadri, Ralte Lalrempuia, Karl W. Törnroos, Erwan Le Roux**

Department of Chemistry, University of Bergen, Allégaten 41, N-5007, Bergen, Norway.

Tel: +47 555 89491; E-mail: Erwan.LeRoux@uib.no

Abstract

Bis-ligated titanium(IV) metal complexes supported by bidentate unsymmetrical *o*-hydroxyaryl-substituted N-heterocyclic carbene ligands were synthesized and structurally identified. While the direct addition of the doubly deprotonated bulky imidazolidinium chloride salts [$^{Dipp,4\text{-}R}$NHC-H]Cl (with Dipp = 2,6-diisopropylphenyl, R = H (2-hydroxyphenyl), and R = Me (2-hydroxy-4-methyl-phenyl)) with chloro-titanium precursor favors the formation of single stereoisomer corresponding to the bis-ligated titanium complexes *trans*-([κ^2-C,O]-$^{Dipp,4\text{-}R}$NHC)$_2$TiCl$_2$ (R = H (2-hydroxyphenyl) for **4a^{H}**, and R = Me (2-hydroxy-4-methyl-phenyl) for **4a^{Me}**), the reactivity with sterically less hindered imidazolidinium chloride salts [^{Mes,H}NHC-H]Cl and [^{Dep,H}NHC-H]Cl as protio-ligands (with Mes = 2,4,6-trimethylphenyl and Dep = 2,6-diethylphenyl) did not afford to single stereoisomer of bis-ligated titanium complexes. These results combined with topographic steric maps as well as the buried volume descriptor (%V_{bur}) indicate that bidentate bulky *N*-Dipp-substituted NHC ligands offer some level of steric protection preventing the formation of other possible bis-ligated (C,O)-NHC-titanium stereoisomers.

Keywords

Titanium; Bidentate ligand; Unsymmetrical N-heterocyclic carbene; Bis-ligated titanium complex; Ethylene polymerization.

1. Introduction

Since the first isolation and characterization of the *N*-heterocyclic carbene (NHC) by Bertrand [1] and Arduengo [2], NHCs have gained outstanding importance as ancillary ligands throughout most of the late transition metals and provided an useful hand of robust and versatile organometallic compounds for homogeneous catalysis [3]. Although late transition metal complexes show strong metal carbene bonds and slow dissociation with most of the NHC ligands, many of the early transition and *f*-block metals show the opposite trend [4]. Thus, to reduce the tendency of the NHC to dissociate from transition metal, considerable research effort have been devoted toward the studies of multidentate anionic carbon, nitrogen, oxygen and sulfur functionalized-NHC ligands [3h, 5]. A series of anionic carbon (i.e. phenyl, cyclopentadienyl, indenyl, fluorenyl), nitrogen (i.e. amido), oxygen (i.e. alkoxide, aryloxide, enolate) and sulfur (thiolate) groups have been developed to act as tethers for holding the NHC moiety in a close proximity to oxophilic metal centers [3f, h, 4b, d, 4f-h]. For example, the use of multidentate oxygen-functionalized NHC ligands of group 4 has proven to be an effective synthetic method for developing robust catalysts for the oligomerization and (co-)polymerization of olefins [6], hydroamination/cyclization of primary aminoalkenes [7], ring-opening polymerization (ROP) of *rac*-lactide [8], and selective coupling of epoxides and CO_2 to either polycarbonates [9] or cyclic carbonates [9b]. Of particular interest, the bidentate *o*-hydroxyaryl substituted NHCs are structurally analogous to bidentate salicylaldimine ligands [10], and are amongst the most commonly studied ligand classes in coordination chemistry due to their ease of preparation, ability to stabilize various metals in different oxidation states, and particularly valuable for the fine-tuning of electronic and steric parameters in a large variety of catalytic organic and polymerization reactions [11]. Recent investigations on bis-ligated bidentate alkoxy/aryloxy-functionalized NHCs of group 4, when activated by MAO (methylaluminoxane), showed to be active in ethylene [6d, f, g, l], ethylene/1-octene and ethylene/norbordene [6d] (co-)polymerization, and stereoselective in propylene [6f, g] and styrene polymerization [6l] similarly to the class of salicylaldimine group 4 catalysts (aka phenoxy-imine, FI, Chart 1) [11e]. Following these leads, we sought to use bidentate *o*-hydroxyaryl substituted NHC-based ligands framework that are analogous to FI ligands in efforts to conceive a new class of catalysts not only for olefins polymerization, but also for the copolymerization of CO_2 and cyclohexene oxide (CHO) in order to extend our studies on active and highly selective catalysts based on tridentate bis(aryloxy) NHC ligand sets of group 4 [9]. In addition to complex developed by Grubbs, *i.e. cis*-([κ^2-C,O]-$^{Dipp,(3\text{-}Ad,5\text{-}Me)}$NHC)$_2$TiCl$_2$ (with 3-Ad, 5-Me = (2-hydroxy-3-(adamant-1-yl)-5-methylphenyl), and a Dipp moiety as *N*-aryl substituent, Chart 1) [6d][6l], a similar set of unsymmetrical *o*-hydroxyaryl NHC ligands was synthesized bearing sterically less-hindered substituents on the *N*-aryloxy moieties and with various *N*-aryl substituents such as Dipp, Mes and Dep groups, as well as their coordination behavior to titanium. Preliminary data concerning the ability of the isolated bis-ligated (C,O)-NHC-titanium complexes to initiate the ethylene polymerization are also presented.

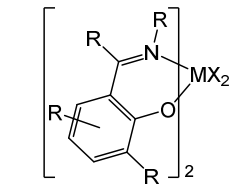

M = group 4 (FI catalysts)

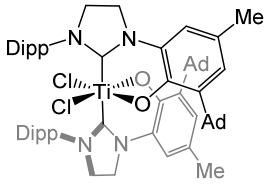

cis bis-ligated
[κ^2-C,O]-NHC titanium

Chart 1

2. Results and Discussion

*2.1. Synthesis of o-hydroxyaryl substituted imidazolidinium protio-ligands **3a-c***

The *o*-hydroxyaryl substituted imidazolidinium chloride salts [$^{Ar,4\text{-}H}$NHC-H]Cl **3a^{H}** (with Ar = Dipp) and **3c** (with Ar = Mes) were prepared according to the established procedure [12], and [$^{Dipp,4\text{-}Me}$NHC-H]Cl **3a^{Me}** and [$^{Dep,4\text{-}H}$NHC-H]Cl **3b** by adapting this literature procedure: ethyl chlorooxoacetate was reacted in THF with the appropriate arylamine **a-c** in presence of triethylamine at 0 °C to give the corresponding oxanilic acid esters **1a-c**, which were treated with the suitable aminoalcohols to afford quantitatively to oxalamides **2a-c** (Scheme 1). Subsequent reduction of **2a-c** with borane THF-adduct and acidification of ethylenediamine moieties followed by their cyclization with an excess of triethyl orthoformate affords to imidazolidinium protio-ligands **3a-c** in high overall yields (Scheme 1). Protio-ligand **3c** was further characterized by X-ray crystallography and crystallizes as a well-separated ion pair as found in other analogous imidazolidinium salt (Fig. S1, Table S1-3) [13]. The ^{1}H NMR spectra of imidazolidinium salt [$^{Dipp,4\text{-}Me}$NHC-H]Cl **3a^{Me}** and [$^{Dep,4\text{-}H}$NHC-H]Cl **3b** display the characteristic chemical resonances of the C*H*$_{imidazolidinium}$ proton (singlet at δ 9.05 and 8.96 ppm, respectively) and two broad triplets for the NC*H*$_2$ protons (apparent A_2B_2 system) of the *o*-hydroxyaryl unsymmetrically substituted imidazolidinium ring (centered at δ 4.59 ppm with υ_{AB} = 192 Hz and 4.64 ppm with υ_{AB} = 216 Hz, respectively), which are well-in-line with the reported data for **3a^{H}** and **3c** (Fig. S2-3) [12]. The ^{13}C NMR spectra of **3a^{Me}** and **3b** show typical chemical resonances at δ 156.6 and 157.2 ppm in chloroform-*d*, respectively, corresponding to the CH$_{imidazolidinium}$ carbons (Fig. S4-5). The IR spectra of both protio-ligands also exhibit stretches at 1624 ($\nu_{C=N}$) cm^{-1} characteristic of the imidazolidinium ring.

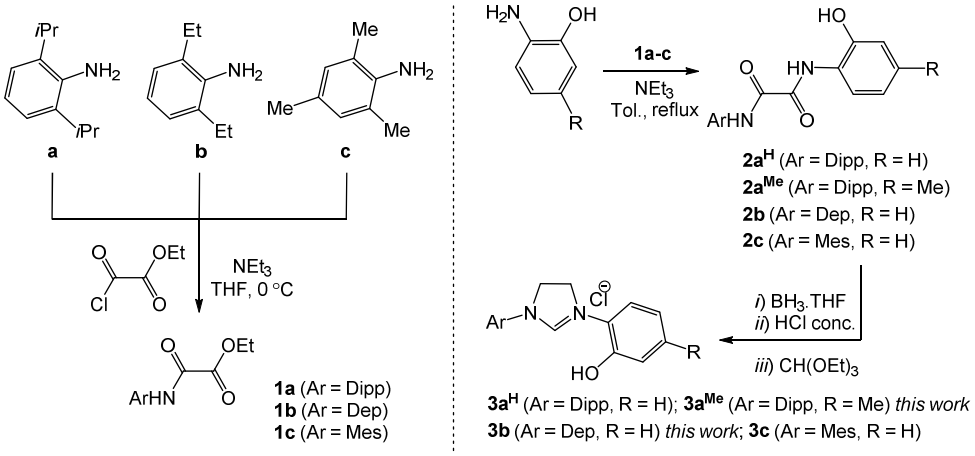

Scheme 1. Synthetic route for unsymmetrical *o*-hydroxyaryl substituted imidazolidinium salts **3a-c** [12].

2.2. Synthesis of bis-ligated o-hydroxyaryl substituted NHC titanium complexes ***4a^{H}*** *and* ***4a^{Me}***

Following the synthetic route reported previously by Grubbs [6d], the *o*-hydroxyaryl substituted imidazolidinium salts **3a^{H}** and **3a^{Me}** were doubly deprotonated by two equivalent of potassium bis(trimethylsilyl)amide (Kbtsa) for 10 min before to be treated with a 1M solution of $TiCl_4$ in toluene for 1 h affording to complexes **4a^{H}** and **4a^{Me}** as dark-red solids in quantitative yield (Scheme 2). Attempts using other synthetic methods for the syntheses of NHC-group 4 complexes [8b, 9a-c], such as the direct addition of imidazolidinium salts to Ti(O*i*Pr)$_4$ (alcohol elimination route) under different temperature conditions (room temperature to reflux) and solvents (toluene, THF), which should give in principle similar compounds, did not lead to the bis-ligated titanium complexes. It is interesting to note that the addition of one equivalent of deprotonated imidazolidinium salts **3a^{H}** or **3a^{Me}** to $TiCl_4$ mainly leads to the formation of bis-ligated NHC complexes of titanium as major products. The ^{1}H NMR spectra of **4a^{H}** and **4a^{Me}** show similar pattern, *i.e.* the disappearance of C$H_{\text{imidazolidinium}}$ proton and the appearance of a centrosymmetric multiplet assigned to the magnetically nonequivalent NCH_2 protons (geminal AA'BB' system) on the NHC ring, which is consistent with either a C_{2h} or C_{2v}-symmetry molecule in solution (Fig. S6-7). The ^{13}C NMR spectra of both complexes **4a^{H}** or **4a^{Me}** confirm the NHC$_{\text{carbene}}$ ligation to the titanium central atom with typical chemical resonances of the carbene at δ 206.7 and 206.6 ppm in benzene-d_6, respectively, (Fig. S8-9) [4g].

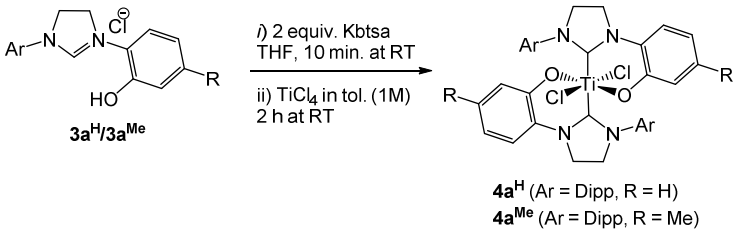

Scheme 2. Syntheses of bis-ligated *o*-hydroxyaryl NHC titanium complexes.

Single crystals of **4a^{H}** were obtained after few days from a saturated solution of the complex in dichloromethane at -30 °C. The molecular structure of **4a^{H}** was determined by single-crystal X-ray diffraction that confirms the chelation of two aryloxide-NHC ligands to titanium (Fig. 1). Compound **4a^{H}** crystallizes in the space group $P2_1/n$, corresponding to a C_{2h}-symmetry molecule which is consistent with the observed ^{1}H NMR spectroscopy in solution. As depicted in figure 1, the structure determined for **4a^{H}** shows that the titanium center adopts a nearly perfect octahedral geometry (Table 1). As previously reported for similar bis-ligated NHC titanium complex, *i.e. cis*-([κ^2-C,O]-$^{Dipp,(3\text{-}Ad,5\text{-}Me)}$NHC)$_2$TiCl$_2$ [6d], the two neutral NHC moieties are in *trans* position to each other (∠C$_{carbene}$-Ti-C$_{carbene}$ = 180.00(8)°) for complex **4a^{H}** and for the complex *cis*-([κ^2-C,O]-$^{Dipp,(3\text{-}Ad,5\text{-}Me)}$NHC)$_2$TiCl$_2$) at 178.0(9)° occupying the axial positions (Table 1 and Table S4-5). However unlike complex *cis*-([κ^2-C,O]-$^{Dipp,(3\text{-}Ad,5\text{-}Me)}$NHC)$_2$TiCl$_2$ having both two oxygen and two chloride atoms located in *cis* position (∠O$_{Ar}$-Ti-O$_{Ar}$ = 88.35(7)° and ∠Cl-Ti-Cl = 96.04(3)°, respectively), complex **4a^{H}** has the two oxygen and two chloride atoms in *trans* to each other (∠O$_{Ar}$-Ti-O$_{Ar}$ = 180.0° and ∠Cl-Ti-Cl = 180.0°). Contrary to complex *cis*-([κ^2-C,O]-$^{Dipp,(3\text{-}Ad,5\text{-}Me)}$NHC)$_2$TiCl$_2$ (which crystallizes as a C_2-symmetry molecule, enantiomer Λ), where the *cis*-configuration is favored to avoid the steric repulsion between Dipp and bulky Ad substituents [6d], complex **4a^{H}** is lacking of such bulky substituents, and thus leading to the most thermodynamically stable *trans* configuration as recently demonstrated by density functional theory calculation on bis-ligated alkoxy-functionalized NHC-Zr systems [6f, g]. Due to the more effective way that both NHC ligands wrap around titanium in **4a^{H}** in this *trans*-configuration, the overall bond lengths (*i.e.* Ti-C$_{carbene}$, and at least one of -Cl and –O bonds) are shorter, and one of the bite angles (∠O$_{Ar}$-Ti-C$_{carbene}$) is larger with a less pronounced deviation from planarity (∠O$_{Ar}$–C$_{Ar}$–N–C$_{carbene}$) for one of the NHC ligands compared to the complex *cis*-([κ^2-C,O]-$^{Dipp,(3\text{-}Ad,5\text{-}Me)}$NHC)$_2$TiCl$_2$ (Table 1).

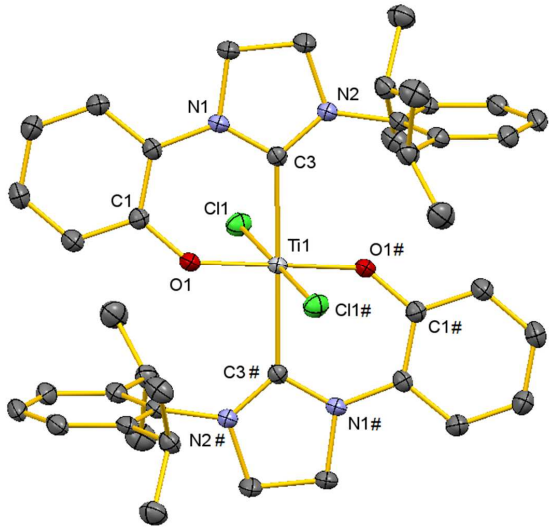

Fig. 1 Crystal structure of compound **4a^{H}** with anisotropic displacement parameter's set at the 50% probability level. Hydrogen atoms and a co-crystallized solvent dichloromethane molecule are omitted for clarity. Selected bond distances, bond angles and torsions angles are listed in table 1. Symmetry code #: 1-x+1, -y+1, -z+1.

Table 1

Selected Bond Distances, Bond Angles and Torsion Angles for Bis-Ligated ([κ^2-C,O]-^{Dipp,R}NHC)$_2$TiCl$_2$ complexes.

	trans-([κ^2-C,O]-$^{Dipp,4\text{-}H}$NHC)$_2$TiCl$_2$ (**4a^{H}**)	*cis*-([κ^2-C,O]-$^{Dipp,(3\text{-}Ad,5\text{-}Me)}$NHC)$_2$TiCl$_2$[a]
Bond lengths (Å)		
Ti-$C_{carbene}$	2.2597(18)/2.2597(18)	2.264(3)/2.275(3)
Ti-O_{Ar}	1.8578(12)/1.8579(12)	1.870(1)/1.842(1)
Ti-Cl	2.3269(5)/2.3269(5)	2.337(8)/2.297(6)
Bond Angles (deg)		
$C_{carbene}$-Ti-$C_{carbene}$	180.00(8)	178.0(9)
O_{Ar}-Ti-O_{Ar}	180.0	88.35(7)
O_{Ar}-Ti-$C_{carbene}$	82.40(6)/82.40(6)	82.45(8)/80.43(8)
Cl-Ti-Cl	180.0	96.04(3)
O_{Ar}-Ti-Cl	90.71(4)/89.29(4)	169.14(5)/88.32(5)
$C_{carbene}$-Ti-Cl	84.73(4)/95.27(4)	88.15(6)/83.54(6)
Torsion Angles (deg)		
O_{Ar}–C_{Ar}–N–$C_{carbene}$[b]	10.65/-10.65	1.95/-19.21

[a] Ref. [6d].

[b] O_{Ar}–C_{Ar}–N–$C_{carbene}$: O1–C1–N1–C3/O1#–C1#–N1#–C3# for **4a^{H}** and O1–C21–N2–C1/O2–C53–N4–C33.

Although the steric hindrance could be conceptualized for both *trans* and *cis* bis-ligated complexes, the availability of solid-state molecular structures allows to calculate the percent buried volume (%V_{bur}, *via* Samb*V*ca 2.0 calculations) and visualize the steric maps for further comparisons of each substituents on NHC ligands [14]. To make a best comparison of both complexes, the analyses were made only by considering ([κ²-C,O]-NHC)-Ti moiety and assuming a 3.5 Å radius of the sphere around the titanium for a Ti–$C_{carbene}$ length of 2.26 Å. Figure 2 shows minor differences between the two unsymmetrical NHC moieties with nearly identical steric map and %V_{bur} (37.0 *vs.* 36.5); thus, making it difficult to appreciate the steric profiles of these ligands using a value of 3.5 Å, which best defines the steric hindrance in the first coordination sphere around the metal. The differences between those two ligands become more marked when increasing the spherical radius around the metal to 5.0 Å allowing taking in account the bulky groups not bound to the metal. The C_{2h}-symmetry steric map of the NHC ligand in **4a^{H}**, with %V_{bur} of 33.4, shows a rather flat steric map with two small bulges located in the northern and western quadrants (corresponding to the *i*Pr groups of *N*-Dipp substituent), and two large hollows which can easily accommodate two Cl atoms in *trans* to each other in the empty southern (SW, SE) and northern quadrants (NE). In contrast, the C_2-symmetry steric map of *cis*-([κ²-C,O]-$^{Dipp,(3\text{-}Ad,5\text{-}Me)}$NHC)$_2$TiCl$_2$ with %V_{bur} of 38.0 shows a non-flat steric map particularly in the south-eastern quadrant imposed by the upward-pointing Ad substituent and two narrow hollows (SW and NE quadrants). From these steric maps, it is clear that the *trans*-configuration observed in these bis-ligated titanium complexes (**4a^{H}** and **4a^{Me}**) is largely favored by the embedment of the second NHC ligand bearing a H as *ortho* substituent on the aromatic ring, and when replaced by the more hindered Ad substituent, only the *cis*-configuration with the second Ad substituent pointing downward (SW quadrant) is allowed among other configurations.

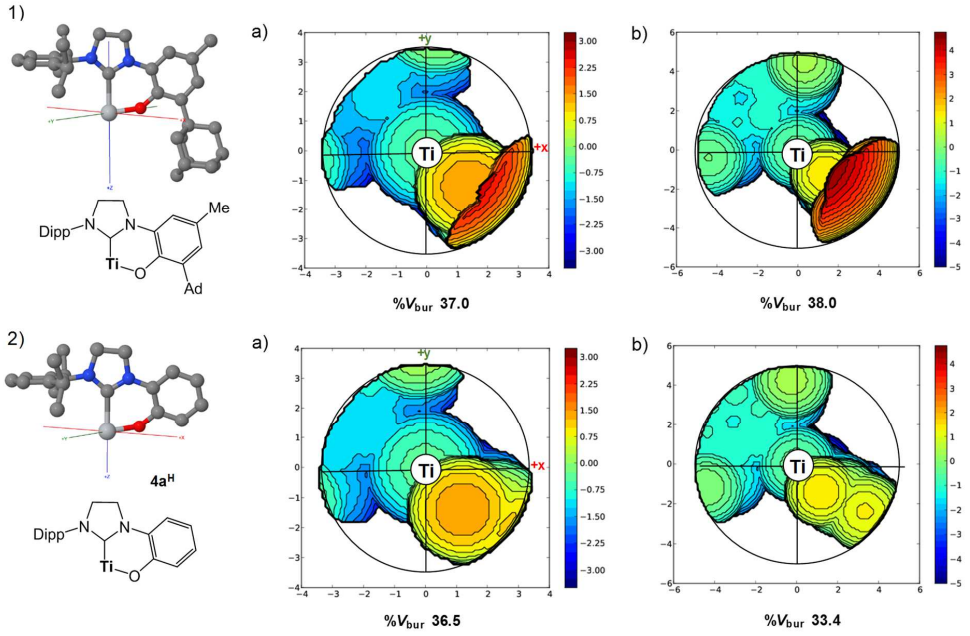

Fig. 2 Ball-and-stick representations and schemes (left) of bidentate ([κ²-C,O]-NHC)-Ti moiety: 1) from *cis*-([κ²-C,O]-$^{Dipp,(3\text{-}Ad,5\text{-}Me)}$NHC)$_2$TiCl$_2$ [6d] and 2) from complex **4a^{H}** with their respective steric maps (right) calculated with a sphere radius of: a) 3.5 Å and b) 5.0 Å [15]. The steric maps of these complexes are oriented in a Cartesian frame with a transverse xy-plane and a +z-axis pointing upward.

Following the same synthetic route described for the aforementioned complexes **4a^{H}** and **4a^{Me}**, the doubly deprotonated *o*-hydroxyaryl imidazolidinium salts **3b** and **3c** protio-ligands bearing less sterically hindered *N*-substituents (Dep and Mes, respectively) were treated by a solution of $TiCl_4$ consistently giving an intractable mixture of products. Although the disappearance of C*H*$_{imidazolidinium}$ and hydroxyl protons were observed for both mixtures in their respective ^{1}H NMR spectra, there are numerous overlapping multiple sets of signals which cannot straightforwardly be assigned but indicates that there are possibly formation of several stereoisomers. In order to rationalize the unsuccessful products isolation, we envisage that the steric map and the calculated %V_{bur} based on our modified X-ray data obtained for **4a^{H}** could adequately mimic the *N*-Mes substituent, *i.e.* by replacing the *i*Pr groups from the *N*-Dipp substituent by Me groups and give an insight trend of reactivity (Fig. 3). Interestingly, the simulated steric map of this bidentate NHC bearing *pseudo N*-Mes' substituent is substantially flat for both sphere radii of 3.5 and 5 Å in the NW and SE quadrants (with largely inferior %V_{bur}), with two large hollows in the adjacent quadrants. Through these steric maps and the previous ones, it can be deduced that the *ortho* bulky *i*Pr groups on the *N*-Dipp are the steric driving force leading mostly to *trans*-configuration complexes (in absence of *ortho* bulky group on the aromatic ring). When those *N*-aryl substituents are exchanged by less bulky groups (here Me), there is a drastic lack of steric hindrance to inhibit the formation of several species, which is leading most likely in our case, to the formation of many stereoisomers.

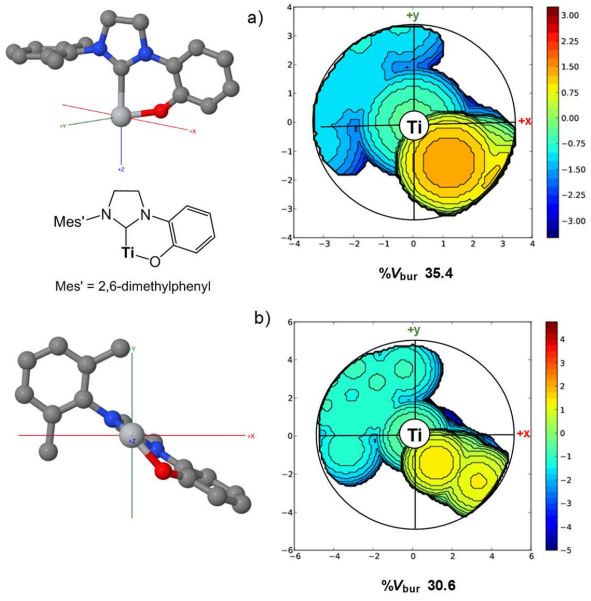

Fig. 3 Ball-and-stick representation, scheme (left) and projection (right) of the simulated steric map for a bidentate ([κ²-C,O]-$^{Mes',4\text{-}H}$NHC)-Ti moiety with a sphere radius of a) 3.5 Å and b) 5.0 Å [15]. The steric maps of these complexes are oriented in a Cartesian frame with a transverse xy-plane and a +z-axis pointing upward.

2.3. Polymerization Studies

Following previous studies on the copolymerization of epoxides and CO_2 catalyzed by group 4 metal complexes bearing benzotriazole alkoxide [16], bis(salphen) [17] ligands, showing structural similarities with our current 6-coordinate bis-ligated bidentate aryloxy NHC titanium complexes, and the highly selective catalysts based on the tridentate bis-aryloxy NHC complexes of group 4 [9a, c], we were interested in evaluating these complexes in the copolymerization of epoxides with CO_2. Copolymerization experiments of CHO with CO_2 were performed by using **4a^{H}**, **4a^{Me}** and *cis*-([κ²-C,O]-$^{Dipp,(3\text{-}Ad,5\text{-}Me)}$NHC)$_2$TiCl$_2$ compounds in the presence of most common co-catalysts such as [PPN]Cl, [PPN]N_3 and[Bu_4N]Cl to form the putative anionic catalysts [9]. The copolymerization of neat CHO with CO_2 shows no polycarbonate formation (conditions: 1 bar of CO_2 at 60 °C, ratio CHO:Ti = 2500) or other side-products such as cyclohexene carbonate or poly(cyclohexene oxide) ring-opening polymerization of CHO. The absence of activity is probably due to the steric congestion around the metal center and/or high stability avoiding the association of the co-catalysts nucleophile to form the "activated" species [9a, c] and/or the epoxide.

Due to the previous studies based on (non-)metallocene and phenoxy-imine catalysts development and their impact on the coordination polymerization of olefins for shaping tailored microstructure of polymers or synthetizing oligomers [11e, 18], systems based on functionalized NHC group 4 catalysts, especially the ones bearing multidentate and asymmetric auxiliary NHC ligands, have been recently explored for the α-olefins polymerization [6a-g, 6l, 19] and 1-hexene trimerization catalysis [6j]. More recently, a series of *C*$_2$-symmetric bidentate *o*-hydroxyaryl unsymmetrically substituted NHC ligands of group 4 were found moderately active in ethylene [6d, f, g, l], ethylene/1-octene and ethylene/norbordene [6d] (co-)polymerization , and stereoselective in propylene (isotactic up to ca. 70%) [6f, g] and styrene (syndiotactic up to ca. 99% in *rrrrrr* heptads) polymerization [6l]. The preliminary reported performance on *C*$_2$-symmetric and sterically hindered *cisoid* catalyst (*cis*-([κ²-C,O]-$^{Dipp,(3\text{-}Ad,5\text{-}Me)}$NHC)$_2$TiCl$_2$) in (co)polymerization show moderate and excellent stereoselectivity in α-olefins polymerization [6d, l], we were interested to evaluate the performance of the sterically less hindered **4a^{H}** and **4a^{Me}** catalysts with different spatial configuration (*transoid*). Thus, next to the *cis*-([κ²-C,O]-$^{Dipp,(3\text{-}Ad,5\text{-}Me)}$NHC)$_2$TiCl$_2$ catalyst, the newly synthesized compounds **4a^{H}** and **4a^{Me}** were examined for ethylene polymerization in the presence of 500 equiv. of MAO as co-catalyst. The preliminary polymerization results show that *trans*-**4a^{H}** and **4a^{Me}** catalysts have a moderate overall activity: 1206 and 1453 g_{PE} $mmol_{Ti}^{-1}$ h^{-1} (conditions: 40 bar of ethylene at room temperature and quenched after 5 min.), respectively, which are comparable to other group 4 systems [11e, 18]. However, the activities of both catalysts remain slightly superior to the benchmark catalyst *cis*-([κ²-C,O]-$^{Dipp,(3\text{-}Ad,5\text{-}Me)}$NHC)$_2$TiCl$_2$ (1131 g_{PE} $mmol_{Ti}^{-1}$ h^{-1}) under similar conditions [6d, l]. The difference in activity in this case is mostly assigned to the extremely bulky bidentate aryloxy NHC ligand wrapping the titanium center, notably with its Ad

substituent retarding the ethylene association to the metal rather than the *cis*/*transoid* configuration itself.

3. Conclusions

In summary, we have successfully synthesized a set of *o*-hydroxyaryl-substituted NHC ligands and the corresponding bis(aryloxide-NHC) titanium complexes. The bulky *N*-aryl substituent (such as Dipp *vs.* Mes and Dep) at the NHCs combined with the other *ortho*-substituent on the *N*-aryloxy moieties appear essential for leading to a single stereoisomer. Meaning that both steric factors have a significant effect on the configuration (*trans* or *cis*) of the final bis-ligated titanium complex, which can be fine-tuned by varying the size of the *N*-functional groups on the NHCs. The *cis*-bis(aryloxide-NHC) titanium complexes show moderate catalytic activities in ethylene polymerization, and the *N*-substituents at the NHCs and the configurations of the complexes have modest effect on the activity.

4. Experimental

4.1. General procedures

All operations were performed with rigorous exclusion of air and water, using standard Schlenk, high-vacuum and glovebox techniques (MB Braun MB200B-G; <1 ppm O_2, <1 ppm H_2O). Dichloromethane, hexane, THF and toluene were purified by using Grubbs columns (MB Braun Solvent Purification System 800). Benzene-d_6 and chloroform-*d* (99.96%) were obtained from Aldrich, dried over sodium or CaH_2, vacuum transferred, degassed and filtered prior to use. All other chemicals were purchased from Aldrich and used as received. The oxanilic acid ethyl esters (**1a** and **1c**), oxalamides (**2a^{H}** and **2c**), unsymmetrical *o*-hydroxyaryl substituted imidazolidinium chloride salts (**3a^{H}** and **3c**) and (*cis*-[κ^2-C,O]-$^{Dipp,3\text{-}Ad/5\text{-}Me}$NHC)$_2$TiCl$_2$ were prepared according to the literature procedures [6d, 12]. The imidazolidinium chloride salt **3c** was crystallized from acetonitrile/hexane (1/5) at -30 °C (CCDC reference code 1579164). The NMR spectra of air and moisture sensitive compounds were recorded using J. Young valve NMR tubes at 298 K on a *Bruker*-AVANCE-DMX400 spectrometer (5 mm BB, ^{1}H: 400.13 MHz; ^{13}C: 100.62 MHz) and a *Bruker*-BIOSPIN-AV500 and AV600 (5 mm BBO, ^{1}H: 500.13 MHz; ^{13}C: 125.77 MHz and 5 mm triple resonance inverse CryoProbe, ^{1}H: 600.13 MHz; ^{13}C: 150.91 MHz). ^{1}H and ^{13}C shifts are referenced to internal solvent resonances and reported in *parts per million* (ppm) relative to TMS. IR spectra were recorded on a Nicolet FT-IR Protégé 460 spectrometer with a DRIFT collector. The spectra were averaged over 64 scans; the resolution was ±4 cm^{-1}. Elemental analyses of C, H and N were performed on an Elementar Vario EL III instrument.

4.2. Unsymmetrical o-hydroxyaryl-substituted imidazolidinium protio-ligand syntheses

*4.2.1. 1-(2,6-diisopropylphenyl)-3-(2-hydroxy-4-methylphenyl)-4,5-dihydro-imidazolyl chloride salt (**3a^{Me}**)*

Compound *N*-(2,6-diisopropylphenyl)-oxanilic acid ethyl ester **1a** (1.71 g, 6.15 mmol) and 2-amino-5-methylphenol (1 equiv., 758 mg, 6.15 mmol) were dissolved in toluene (100 mL), and 0.86 mL of NEt_3 (1 equiv., 6.15 mmol) was added under inert atmosphere. The suspension was stirred and heated to reflux overnight. After cooling down the solution, a precipitate was obtained which was dissolved in EtOAc. The solution was washed with 2 M HCl (2x100 mL). The aqueous phase was then washed with EtOAc and the combined organic phases were washed with brine, dried over $MgSO_4$ and dried under vacuum. The solid was crystallized from warm toluene to afford *N*-(2,6-diisopropylphenyl)-*N'*-(2-hydroxy-4-methylphenyl)-oxalamide **2a^{Me}** (1.47 g, 67% yield). ^{1}H NMR (400.13 MHz, chloroform-*d*): δ 9.56 (s, 1H, N*H*), 8.81 (s, 1H, N*H*), 8.25 (s, 1H, O*H*), 7.37 (t, *J* = 7.8 Hz, 1H, Ar$_{Dipp}$-*H*), 7.24 (d, *J* = 8.2 Hz, 2H, Ar-*H*), 7.23 (d, *J* = 7.8 Hz, 1H, Ar$_{Dipp}$-*H*), 6.84 (s, 1H, Ar-*H*), 6.74 (d, *J* = 8.2 Hz, 1H, Ar-*H*), 3.02 (sept., *J* = 6.9 Hz, 2H, C*H*(CH_3)$_2$), 2.32 (s, 3H, Ar-C*H*$_3$), 1.22 (d, *J* = 6.9 Hz, 12H, CH(C*H*$_3$)$_2$) ppm.
Under inert atmosphere, to compound **2a^{Me}** (1.47 g, 4.15 mmol) was added 33.2 mL BH_3-THF (8 equiv., 1M in THF) and the mixture was heated to reflux overnight. After cooling down to room temperature, MeOH was added to the reaction mixture until gas evolution cease and then quenched by ≈ 1.5 mL of conc. HCl. The mixture was dried, dissolved in MeOH and these steps were repeated two more times. To this pale pink solid was added 15 mL of triethyl orthoformate and the solution was stirred at room temperature overnight. The solid was filtered off, washed with Et_2O and dried under vacuum to afford **3a^{Me}** as a white solid (1.20 g, 78% yield).^{1}H NMR (500.13 MHz, chloroform-*d*): δ 9.05 (s, 1H, NC*H*N), 7.47 (t, *J* = 7.8 Hz, 1H, Ar$_{Dipp}$-*H*), 7.35 (s, 1H, Ar-*H*), 7.24 (d, *J* = 7.8 Hz, 2H, Ar$_{Dipp}$-*H)*, 6.95 (d, *J* = 7.8, 1H, Ar-*H*), 6.62 (d, *J* = 7.8 Hz, 1H, Ar-*H*), 4.84 (bm, 2H, NC*H*$_2$), 4.36 (bm, 2H, NC*H*$_2$), 3.00 (sept., *J* = 6.8 Hz, 2H, C*H*(CH_3)$_2$), 2.18 (s, 3H, Ar-C*H*$_3$), 1.28 (d, *J* = 6.8 Hz, 6H, CH(C*H*$_3$)$_2$), 1.17 (d, *J* = 6.8 Hz, 6H, CH(C*H*$_3$)$_2$) ppm. ^{13}C NMR (125.77 MHz, chloroform-*d*): δ 156.6 (NCHN), 149.6 (*C$_{ipso}$*, O-Ar), 146.6 (*C$_q$*, Ar), 139.3 (*C$_q$*, Ar), 131.5 (*C$_q$*, Ar), 130.0 (*C$_q$*, Ar), 125.1 (*C*H, Ar), 120.5 (*C*H, Ar), 120.1 (*C*H, Ar), 119.8 (*C*H, Ar), 119.1 (*C*H, Ar), 52.5 (NCH_2), 51.0 (NCH_2), 28.9 (*C*H(CH_3)$_2$), 25.0 (CH(*C*H$_3$)$_2$), 24.3 (CH(*C*H$_3$)$_2$), 21.1 (Ar-*C*H$_3$) ppm. DRIFT (ν/cm^{-1}): 2970s, 2958s, 2868s, 1624vs, 1588w, 1553w, 1526w, 1494w, 1476w, 1457m, 1420m, 1385w, 1368w, 1335w, 1311m, 1292s, 1283m, 1263s, 1185w, 1166w, 945w, 879w, 812m, 764w, 593w, 487w, 456w. Anal. Calcd for $C_{22}H_{29}ClN_2O$: C, 68.98; H, 7.01; N 8.47. Found: C, 69.16; H, 7.26; N, 8.40.

*4.2.2. 1-(2,6-diethylphenyl)-3-(2-hydroxyphenyl)-4,5-dihydro-imidazolyl chloride (**3b**)*

2,6-diethylaniline (10 mL, 60.7 mmol) and triethylamine (1 equiv., 8.5 mL, 60.7 mmol) were dissolved in dry THF (80 mL). After cooling down the solution at 0 °C, 6.8 mL of ethyl chloroacetate (1 equiv., 60.7 mmol) was added dropwise leading to a formation of smoke and white solid. The solution was allowed to warm up at room temperature and stirred overnight. The solid was filtered off and the organic phase was washed with HCl 2M (2x100 mL). The aqueous phase was then washed with EtOAc and the combined organic phases were washed with brine, dry over $MgSO_4$ and dry under vacuum to afford *N*-(2,6-diethylphenyl)-oxanilic acid ethyl ester **1b** as white solid (11.23

g, 75% yield). ^{1}H NMR (500.13 MHz, chloroform-*d*): δ 8.40 (s, 1H, N*H*), 7.27 (t, *J* = 7.6 Hz, 1H, Ar$_{Dep}$-*H*), 7.15 (d, *J* = 7.6 Hz, 2H, Ar$_{Dep}$-*H*), 4.44 (q, *J* = 7.2 Hz, 2H, O-C*H*$_2$-CH$_3$), 2.59 (q, *J* = 7.6 Hz, 4H, C*H*$_2$-CH$_3$), 1.45 (t, *J* = 7.2 Hz, 3H, O-CH$_2$-C*H*$_3$), 1.20 (t, *J* = 7.6 Hz, 6H, CH$_2$-C*H*$_3$) ppm. ^{13}C NMR (125.77 MHz, chloroform-*d*): δ 161.0 (*C*O, carbimide), 155.4 (*C*O, ester), 141.1 5 (C_q, Ar), 130.9 (C_q, Ar), 128.6 (CH, Ar), 126.5 (CH, Ar), 63.7 (CH$_2$, O-*C*H$_2$-CH$_3$), 24.8 (CH$_2$, *C*H$_2$-CH$_3$), 14.3 (CH$_3$, O-CH$_2$-*C*H$_3$), 14.0 (CH$_3$, CH$_2$-*C*H$_3$) ppm.

Compound **1b** (10.96 g, 43.57 mmol) and 2-aminophenol (1 equiv., 4.80 mg, 43.97 mmol) were dissolved in toluene (100 mL), and 12.3 mL of NEt$_3$ (1 equiv., 87.9 mmol) was added under inert atmosphere. The suspension was stirred and heated to reflux overnight. After cooling down the solution a precipitate was obtained, which was dissolved in dichloromethane. The solution was washed with 2 M HCl (2x100 mL). The aqueous phase was then washed with dichloromethane and the combined organic phases were washed with brine, dried over MgSO$_4$ and dried under vacuum. The solid was crystallized from warm toluene to afford *N*-(2,6-diethylphenyl)-*N'*-(2-hydroxyphenyl)-oxalamide **2b** (10.06 g, 73% yield). ^{1}H NMR (500.13 MHz, chloroform-*d*): δ 9.68 (s, 1H, N*H*), 8.88 (s, 1H, N*H*), 8.06 (s, 1H, O*H*), 7.50 (dd, *J* = 8.1 Hz, *J* = 1.4 Hz, 1H, Ar$_{Dep}$-*H*), 7.30 (m, 1H, Ar-*H*), 7.18 (s, 1H, Ar$_{Dep}$-*H*), 7.17 (s, 1H, Ar$_{Dep}$-*H*), 7.15 (m, 1H, Ar-*H*), 6.97 (dd, *J* = 8.1 Hz, *J* = 1.4 Hz, 1H, Ar$_{Dep}$-*H*), 6.92 (m, 1H, Ar-*H*), 2.61 (q, *J* = 7.6 Hz, 4H, C*H*$_2$-CH$_3$), 1.21 (t, *J* = 7.6 Hz, 6H, CH$_2$-C*H*$_3$) ppm.

Following the procedure described for **3a^{Me}**, the reaction of **2b** (1.92 g, 6 mmol) and 49.2 mL of BH$_3$-THF (8 equiv., 1M in THF) yielded **3b** (1.6 g, 81% yield) as a white solid. ^{1}H NMR (500.13 MHz, chloroform-*d*): δ 8.96 (s, 1H, NC*H*N), 7.57 (d, *J* = 8.2 Hz, 1H, Ar$_{Dep}$-*H*), 7.41 (t, *J* = 7.8 Hz, 1H, Ar-*H*), 7.20 (d, *J* = 7.8 Hz, 2H, Ar$_{Dep}$-*H*), 7.10 (d, *J* = 7.8 Hz, Ar-*H*), 6.96 (t, *J* = 7.7 Hz, 1H, Ar-*H*), 6.77 (t, *J* = 7.7 Hz, 1H, Ar-*H*), 4.86 (bt, *J* = 10.4 Hz, 2H, NC*H*$_2$), 4.42 (bt, *J* = 10.4 Hz, 2H, NC*H*$_2$), 2.64 (q, *J* = 7.5 Hz, 4H, C*H*$_2$-CH$_3$), 1.22 (t, *J* = 7.5 Hz, 6H, CH$_2$-C*H*$_3$) ppm. ^{13}C NMR (125.77 MHz, chloroform-*d*): δ 157.2 (NCHN), 150.0 (C_{ipso}, O-Ar), 141.6 (C_q, Ar), 131.8 (C_q, Ar), 131.2 (C_q, Ar), 128.8 (*C*H, Ar), 127.6 (*C*H, Ar), 122.7 (*C*H, Ar), 120.3 (*C*H, Ar), 119.9 (*C*H, Ar), 118.9 (*C*H, Ar), 51.5 (N*C*H$_2$), 51.0 (N*C*H$_2$), 24.3 (CH$_2$, *C*H$_2$-CH$_3$), 15.2 (CH$_3$, CH$_2$-*C*H$_3$) ppm. DRIFT (ν/cm^{-1}): 2971s, 2959s, 2869s, 1624vs, 1588w, 1555w, 1525w, 1494w, 1476w, 1457m, 1421m, 1385w, 1368w, 1337w, 1313m, 1292s, 1284m, 1263s, 1186w, 1166w, 945w, 880w, 812m, 763w, 593w, 487w, 455w. Anal. Calcd for $C_{19}H_{23}ClN_2O$: C, 68.97; H, 7.01; N 8.47. Found: C, 68.79; H, 7.26; N, 8.36.

4.3. Preparation of bis-ligated o-hydroxyaryl substituted NHC titanium(IV) complexes

*4.3.1. 1-(2,6-diisopropylphenyl)-3-(2-hydroxyphenyl)-4,5-dihydro-imidazolyl titanium(IV) dichloride (**4a^H**)*

In a vial 1-(2,6-diisopropylphenyl)-3-(2-hydroxyphenyl)-4,5-dihydro-imidazolyl chloride salt **3a^H** (588.0 mg, 1.64 mmol) and potassium bis(trimethylsilyl)amide (2 equiv., 561.35 mg, 3.27 mmol) were dissolved in THF (3 mL), and the resulting yellow suspended mixture was stirred for 10 min at room temperature. To this mixture was added 0.82 mL of a solution of 1M titanium tetrachloride in toluene (0.5 equiv., 0.82 mmol) in 2 mL THF. The solution rapidly turned dark red and was allowed to stir for 2

h at room temperature. Subsequent centrifugation, filtration and evaporation to dryness afforded complex **4a^{H}** as a dark red solid in quantitative yield. Crystals of **4a^{H}** were obtained from a saturated solution of dichloromethane at -30°C for several days. ^{1}H NMR (500.13 MHz, benzene-d_6): δ 7.42 (t, J = 7.7 Hz, 2H, Ar$_{Dipp}$-H), 7.29 (d, J = 7.7 Hz, 4H, Ar$_{Dipp}$-H), 7.01 (m, 2H, Ar-H), 6.75 (m, 2H, Ar-H), 6.37 (dd, J = 8.1 Hz, J = 1.4 Hz, 2H, Ar-H), 5.26 (dd, J = 8.1 Hz, , J = 1.4 Hz, 2H, Ar-H), 3.47 (sept., J = 6.8 Hz, 4H, CH(CH$_3$)$_2$), 3.07 (m, 4H, NCH_2), 2.95 (m, 4H, NCH_2), 1.56 (d, J = 6.8 Hz, 12H, CH(CH_3)$_2$), 1.10 (d, J = 6.8 Hz, 12H, CH(CH_3)$_2$) ppm. ^{13}C NMR (125.77 MHz, benzene-d_6): δ 206.7 (N*C*N), 155.0 (C$_{ipso}$, O-Ar), 148.0 (C_q, Ar), 137.8 (C_q, Ar), 133.6 (C_q, Ar), 129.2 (*C*H, Ar), 125.3 (*C*H, Ar), 124.0 (*C*H, Ar), 119.3 (*C*H, Ar), 118.1 (*C*H, Ar), 116.7 (*C*H, Ar), 53.9 (N*C*H$_2$), 47.3 (N*C*H$_2$), 28.5 (*C*H(CH$_3$)$_2$), 26.2 (CH(*C*H$_3$)$_2$), 24.8 (CH(*C*H$_3$)$_2$) ppm. DRIFT (ν/cm^{-1}): 3065w, 3031w, 2961s, 2925m, 2867m, 1610m, 1587m, 1495vs, 1474vs, 1429s, 1408s, 1385w, 1363w, 1317s, 1288vs, 1236m, 1123w, 1056w, 996w, 912m, 879m, 806w, 750m, 671m, 640w, 453w, 438w, 418m. Anal. Calcd for $C_{42}H_{50}Cl_2N_4O_2Ti.2CH_2Cl_2$: C, 56.73; H, 5.84; N 6.01. Found: C, 57.04; H, 6.18; N 5.94.

*4.3.2. 1-(2,6-diisopropylphenyl)-3-(2-hydroxy-4-methylphenyl)-4,5-dihydro-imidazolyl titanium(IV) dichloride (**4a^{Me}**)*

Following the procedure described for **4a^{H}**, the reaction of 1-(2,6-diisopropylphenyl)-3-(2-hydroxy-4-mehtylphenyl)-4,5-dihydro-imidazolyl chloride salt **3a^{Me}** (350.8 mg, 0.94 mmol), potassium bis(trimethylsilyl)amide (2 equiv., 375.2 mg, 1.88 mmol) and titanium tetrachloride (0.5 equiv., 0.47 mL, 0.82 mmol) yielded **4a^{Me}** (323 mg, 87% yield) as a dark red solid. ^{1}H NMR (500.13 MHz, chloroform-d): δ 7.53 (t, J = 7.7 Hz, 2H, Ar$_{Dipp}$-H), 7.35 (d, J = 7.7 Hz, 4H, Ar$_{Dipp}$-H), 6.68 (d, J = 8.2 Hz, 2H, Ar-H), 6.50 (dd, J = 8.2 Hz, J = 1.7 Hz, 2H, Ar-H), 4.60 (d, 2H, J = 1.7 Hz, Ar-H), 4.10 (m, 4H, NCH_2), 3.79 (m, 4H, NCH_2), 3.27 (sept., J = 6.8 Hz, 4H, CH(CH$_3$)$_2$), 2.09 (s, 3H, Ar-CH_3), 1.27 (d, J = 6.8 Hz, 12H, CH(CH_3)$_2$), 1.16 (d, J = 6.8 Hz, 12H, CH(CH_3)$_2$) ppm. ^{13}C NMR (125.77 MHz, chloroform-d): δ 205.8 (N*C*N), 153.6 (C$_{ipso}$, O-Ar), 148.0 (C_q, Ar), 137.3 (C_q, Ar), 133.7 (C_q, Ar), 130.7 (C_q, Ar), 129.2 (*C*H, Ar), 125.0 (*C*H, Ar), 120.3 (*C*H, Ar), 118.1 (*C*H, Ar), 115.5 (*C*H, Ar), 54.0 (N*C*H$_2$), 48.0 (N*C*H$_2$), 28.3 (*C*H(CH$_3$)$_2$), 26.2 (CH(*C*H$_3$)$_2$), 24.5 (CH(*C*H$_3$)$_2$), 20.4 (Ar-*C*H$_3$) ppm. ^{13}C NMR (125.77 MHz, benzene-d_6): δ 206.6 (N*C*N), 154.9 (C$_{ipso}$, O-Ar), 148.3 (C_q, Ar), 138.0 (C_q, Ar), 133.6 (C_q, Ar), 131.3 (C_q, Ar), 129.2 (*C*H, Ar), 125.2 (*C*H, Ar), 119.8 (*C*H, Ar), 118.4 (*C*H, Ar), 116.1 (*C*H, Ar), 53.8 (N*C*H$_2$), 53.3 (N*C*H$_2$), 28.4 (*C*H(CH$_3$)$_2$), 26.1 (CH(*C*H$_3$)$_2$), 24.7 (CH(*C*H$_3$)$_2$), 20.7 (Ar-*C*H$_3$) ppm. DRIFT (ν/cm^{-1}): 3064w, 3032w, 2962s, 2925m, 2867m, 1615s, 1572m, 1506s, 1474vs, 1458s, 1420s, 1402s, 1363w, 1319s, 1292vs, 1234m, 1169m, 1147m, 1056w, 1009w, 960m, 909w, 864w, 804m, 760s, 734w, 663m, 590w, 428w, 415m.

4.4. General procedure for ethylene polymerization

In the glovebox, a vial was charged with a stirring bar, Ti catalyst (5 μmol) in 5 mL of toluene and 500 equiv. of MAO, and placed in an autoclave reactor. After addition of 40 bar of ethylene, the reaction was stirred 5 min and the pressure was released before to quench the reaction by 1 mL of acidified MeOH. Volatiles were removed under reduced

pressure, and polymer was washed with isopropanol and dried under vacuum for 2 h at 150 °C. The polymer yield was determined gravimetrically.

4.5. X-ray crystallography and crystal structure determination

Suitable crystals for diffraction experiments were selected in a glovebox and mounted in a minimum of Parabar 10312 oil (Hampton Research) in a nylon loop and then mounted under a nitrogen cold stream from an Oxford Cryosystems 700 series open-flow cryostat. Data collection was done on a Bruker AXS TXS rotating anode system with an APEXII Pt^{135} CCD detector using graphite-monochromated Mo K_α radiation (λ = 0.710 73 Å). Data collection and data processing were done using APEX2[20], SAINT[21], and SADABS[22] version 2012/1,whereas structure solution and final model refinement were done using SHELXS[23] version 2013/1 or SHELXT[24] version 2014/4 and SHELXL[25] version 2014/7. Crystal data: for **4**$^{\mathbf{aH}}$ obtained from a saturated solution in CH_2Cl_2. $C_{42}H_{50}Cl_2N_4O_2Ti.2(CH_2Cl_2)$, M = 931.51, crystal size: 0.125 x 0.100 x 0.050 mm^3, crystal habit/color: prism/dark red, monoclinic, space group $P2_1/n$ (No.14), a = 11.9657(7), b = 12.9163(8), c = 14.5572(9) Å, β = 99.1720(10)°, V = 2221.1(2) $Å^3$, Z = 2, ρ_{calc} = 1.393 $g.cm^{-3}$, $F(000)$ = 972, μ(Mo-K_α) = 0.595 mm^{-1}, λ = 0.71073 Å, T = 103(2) K. The 28755 reflections measured on a Bruker AXS APEXII Ultra CCD area detector system yielded 4739 unique data (2.050 < θ < 26.776°, R_{int} = 0.0485) [4739 observed reflections ($I > 2\sigma(I)$]. Goodness-of-fit on F^2 = 1.037, $R1$ = 0.0350, $wR2$ = 0.0894, R indices (all data) $R1$ = 0.0486, w$R2$ = 0.0980. CCDC reference code 1579165 contains the supplementary crystallographic data for **4**$^{\mathbf{aH}}$. These data can be obtained free of charge from The Cambridge Crystallographic Data Centre via www.ccdc.cam.ac.uk/data_request/cif.

4.6. %V_{Bur} and steric maps calculations

The %V_{Bur} values and steric maps were evaluated with the SambVca 2.0 package [26]. The radius of the sphere around the center atom was set to: 3.5 Å or 5 Å, distance from the center of the sphere: 2.26 Å, mesh spacing: 0.1 Å, H atoms omitted and atom radii: Bondi radii scaled by 1.17, as recommended by Cavallo.

Acknowledgements

The authors acknowledge the University of Bergen, L. Meltzers Høyskolefond (K. W. T.: bursary no. 2017/3273) and the Norwegian Research Council (FRINATEK grant no. 240333) for financial support. Prof. Dr. Nils Åge Frøystein and Dr. Marco Foscato are thanked for their fruitful discussions on NMR spectroscopy and calculations, respectively.

References

[1] A. Igau, H. Grutzmacher, A. Baceiredo, G. Bertrand, J. Am. Chem. Soc. 110 (1988) 6463-6466.

[2] (a) A.J. Arduengo, M. Kline, J.C. Calabrese, F. Davidson, J. Am. Chem. Soc. 113 (1991) 9704-9705; (b) A.J. Arduengo, H.V.R. Dias, R.L. Harlow, M. Kline, J. Am. Chem. Soc. 114 (1992) 5530-5534.
[3] (a) W.A. Herrmann, M. Elison, J. Fischer, C. Köcher, G.R.J. Artus, Angew. Chem., Int. Ed. Engl. 34 (1995) 2371-2374; (b) W.A. Herrmann, Angew. Chem., Int. Ed. 41 (2002) 1290-1309; (c) V. César, S. Bellemin-Laponnaz, L.H. Gade, Chem. Soc. Rev. 33 (2004) 619-636; (d) S.P. Nolan, Editor, N-Heterocyclic Carbenes in Synthesis, Wiley-VCH Verlag GmbH & Co. KGaA, (2006); (e) F. Glorius, Editor, N-Heterocyclic Carbenes in Transition Metal Catalysis, Springer-Verlag Berlin Heidelberg, (2007); (f) S. Díez-González, S.P. Nolan, Coord. Chem. Rev. 251 (2007) 874-883; (g) S. Díez-González, N. Marion, S.P. Nolan, Chem. Rev. 109 (2009) 3612-3676; (h) M. Poyatos, J.A. Mata, E. Peris, Chem. Rev. 109 (2009) 3677-3707; (i) K. Riener, S. Haslinger, A. Raba, M.P. Högerl, M. Cokoja, W.A. Herrmann, F.E. Kühn, Chem. Rev. 114 (2014) 5215-5272; (j) S.P. Nolan, Editor, N-Heterocyclic Carbenes: Effective Tools for Organometallic Synthesis, Wiley-VCH Verlag GmbH & Co. KGaA, (2014); (k) M.N. Hopkinson, C. Richter, M. Schedler, F. Glorius, Nature 510 (2014) 485-496.
[4] (a) D. Bourissou, O. Guerret, F.P. Gabbaï, G. Bertrand, Chem. Rev. 100 (2000) 39-92; (b) S.T. Liddle, I.S. Edworthy, P.L. Arnold, Chem. Soc. Rev. 36 (2007) 1732-1744; (c) D. Pugh, A.A. Danopoulos, Coord. Chem. Rev. 251 (2007) 610-641; (d) D. McGuinness, Dalton Trans. (2009) 6915-6923; (e) L.-A. Schaper, E. Tosh, W.A. Herrmann, RSC Catal. Ser 6 (2011) 166-195; (f) S. Bellemin-Laponnaz, S. Dagorne, Chem. Rev. 114 (2014) 8747-8774; (g) D. Zhang, G. Zi, Chem. Soc. Rev. 44 (2015) 1898-1921; (h) S. Hameury, P. de Fremont, P. Braunstein, Chem. Soc. Rev. 46 (2017) 632-733.
[5] (a) O. Kuhl, Chem. Soc. Rev. 36 (2007) 592-607; (b) L. Benhamou, E. Chardon, G. Lavigne, S. Bellemin-Laponnaz, V. César, Chem. Rev. 111 (2011) 2705-2733.
[6] (a) H. Aihara, T. Matsuo, H. Kawaguchi, Chem. Commun. (2003) 2204-2205; (b) D.S. McGuinness, V.C. Gibson, J.W. Steed, Organometallics 23 (2004) 6288-6292; (c) D. Zhang, Eur. J. Inorg. Chem. 2007 (2007) 4839-4845; (d) A. El-Batta, A.W. Waltman, R.H. Grubbs, J. Organomet. Chem. 696 (2011) 2477-2481; (e) T.G. Larocque, A.C. Badaj, S. Dastgir, G.G. Lavoie, Dalton Trans. 40 (2011) 12705-12712; (f) C. Bocchino, M. Napoli, C. Costabile, P. Longo, J. Polym. Sci. A Polym. Chem. 49 (2011) 862-870; (g) C. Costabile, C. Bocchino, M. Napoli, P. Longo, J. Polym. Sci. A Polym. Chem. 50 (2012) 3728-3735; (h) T.G. Larocque, G.G. Lavoie, J. Organomet. Chem. 715 (2012) 26-32; (i) E. Despagnet-Ayoub, L.M. Henling, J.A. Labinger, J.E. Bercaw, Dalton Trans. 42 (2013) 15544-15547; (j) S. Dagorne, S. Bellemin-Laponnaz, C. Romain, Organometallics 32 (2013) 2736-2743; (k) E. Despagnet-Ayoub, M.K. Takase, L.M. Henling, J.A. Labinger, J.E. Bercaw, Organometallics 34 (2015) 4707-4716; (l) G.M. Miyake, M.N. Akhtar, A. Fazal, E.A. Jaseer, C.S. Daeffler, R.H. Grubbs, J. Organomet. Chem. 728 (2013) 1-5.
[7] (a) J. Cho, T.K. Hollis, T.R. Helgert, E.J. Valente, Chem. Commun. (2008) 5001-5003; (b) J. Cho, T.K. Hollis, E.J. Valente, J.M. Trate, J. Organomet. Chem. 696

(2011) 373-377; (c) T.R. Helgert, T.K. Hollis, E.J. Valente, Organometallics 31 (2012) 3002-3009; (d) S. Barroso, S.R.M.M. de Aguiar, R.F. Munha, A.M. Martins, J. Organomet. Chem. 760 (2014) 60-66; (e) W.D. Clark, J. Cho, H.U. Valle, T.K. Hollis, E.J. Valente, J. Organomet. Chem. 751 (2014) 534-540; (f) W.D. Clark, K.N. Leigh, C.E. Webster, T.K. Hollis, Aust. J. Chem. 69 (2016) 573-582; (g) H.U. Valle, G. Akurathi, J. Cho, W.D. Clark, A. Chakraborty, T.K. Hollis, Aust. J. Chem. 69 (2016) 565-572.
[8] (a) D. Patel, S.T. Liddle, S.A. Mungur, M. Rodden, A.J. Blake, P.L. Arnold, Chem. Commun. (2006) 1124-1126; (b) C. Romain, L. Brelot, S. Bellemin-Laponnaz, S. Dagorne, Organometallics 29 (2010) 1191-1198; (c) C. Romain, B. Heinrich, S.B. Laponnaz, S. Dagorne, Chem. Commun. 48 (2012) 2213-2215; (d) N. Zhao, G. Hou, X. Deng, G. Zi, M.D. Walter, Dalton Trans. 43 (2014) 8261-8272.
[9] (a) C.C. Quadri, E. Le Roux, Dalton Trans. 43 (2014) 4242-4246; (b) J. Hessevik, R. Lalrempuia, H. Nsiri, K.W. Törnroos, V.R. Jensen, E. Le Roux, Dalton Trans. 45 (2016) 14734-14744; (c) R. Lalrempuia, F. Breivik, K.W. Törnroos, E. Le Roux, Dalton Trans. 46 (2017) 8065-8076; (d) Coralie C. Quadri, Ralte Lalrempuia, Julie Hessevik, Karl. W. Törnroos, E.L. Roux, Organometallics (2017) submitted.
[10] M. Calligarir, L. Randaccio, in: G. Wilkinson, R.D. Gillard, J. McCleverty (Eds.) Comprehensive Coordination Chemistry, Pergamon Press Ltd, Oxford, (1987), pp. 723-726.
[11] (a) C. Gennari, U. Piarulli, Chem. Rev. 103 (2003) 3071-3100; (b) H. Gröger, Chem. Rev. 103 (2003) 2795-2828; (c) M. North, D.L. Usanov, C. Young, Chem. Rev. 108 (2008) 5146-5226; (d) E. Wojaczyńska, J. Wojaczyński, Chem. Rev. 110 (2010) 4303-4356; (e) H. Makio, H. Terao, A. Iwashita, T. Fujita, Chem. Rev. 111 (2011) 2363-2449.
[12] A.W. Waltman, R.H. Grubbs, Organometallics 23 (2004) 3105-3107.
[13] N. Stylianides, A.A. Danopoulos, D. Pugh, F. Hancock, A. Zanotti-Gerosa, Organometallics 26 (2007) 5627-5635.
[14] (a) A. Poater, B. Cosenza, A. Correa, S. Giudice, F. Ragone, V. Scarano, L. Cavallo, Chem. – A Eur. J. 2009 (2009) 1759-1766; (b) L. Falivene, R. Credendino, A. Poater, A. Petta, L. Serra, R. Oliva, V. Scarano, L. Cavallo, Organometallics 35 (2016) 2286-2293.
[15] A. Poater, F. Ragone, R. Mariz, R. Dorta, L. Cavallo, Chem. – A Eur. J. 16 (2010) 14348-14353.
[16] (a) C.-K. Su, H.-J. Chuang, C.-Y. Li, C.-Y. Yu, B.-T. Ko, J.-D. Chen, M.-J. Chen, Organometallics 33 (2014) 7091-7100; (b) H.-J. Chuang, B.-T. Ko, Dalton Trans. 44 (2015) 598-607.
[17] M. Mandal, D. Chakraborty, J. Polym. Sci. Part A: Polym. Chem. 54 (2016) 809-824.
[18] (a) V.C. Gibson, S.K. Spitzmesser, Chem. Rev. 103 (2003) 283-316; (b) H.H. Brintzinger, D. Fischer, R. Mülhaupt, B. Rieger, R.M. Waymouth, Angew. Chem. Int. Ed. 34 (1995) 1143-1170; (c) G.W. Coates, Chem. Rev. 100 (2000) 1223-1252;

(d) C. Redshaw, Y. Tang, Chem. Soc. Rev. 41 (2012) 4484-4510; (e) G.J.P. Britovsek, V.C. Gibson, D.F. Wass, Angew. Chem. Int. Ed. 38 (1999) 428-447.
[19] D. Zhang, N. Liu, Organometallics 28 (2009) 499-505.
[20] Bruker-AXS: APEX2. Version 2014.11-0. Madison, Wisconsin, USA. 2014.
[21] Bruker-AXS: SAINT. Version 7.68A. Madison, Wisconsin, USA, 2010.
[22] L. Krause, R. Herbst-Irmer, G.M. Sheldrick, D. Stalke, J. Appl. Crystallogr. 48 (2015) 3-10.
[23] G. M. Sheldrick, XS. Version 2013/1. Georg-August-Universität Göttingen, Göttingen, Germany, 2013.
[24] G. Sheldrick, Acta Crystallogr., Sect. A: Found. Adv. 71 (2015) 3-8.
[25] G. Sheldrick, Acta Crystallogr., Sect. C: Cryst. Struct. Chem. 71 (2015) 3-8.
[26] The %V_{bur} and steric maps were calculated using the web-based SambVca 2.0 program (https://www.molnac.unisa.it/OMtools/sambvca2.0/index.html)

Supporting Information

Steric Factors on Unsymmetrical *O*-hydroxyaryl *N*-Heterocyclic Carbene Ligands Prevailing on the Stabilization of Single Stereoisomer of Bis-Ligated Titanium Complexes

Coralie C. Quadri, Ralte Lalrempuia, Karl. W. Törnroos, Erwan Le Roux*

Department of Chemistry, University of Bergen, Allégaten 41, N-5007, Bergen, Norway.

Tel: +47 555 89491; E-mail: Erwan.LeRoux@uib.no

Content:

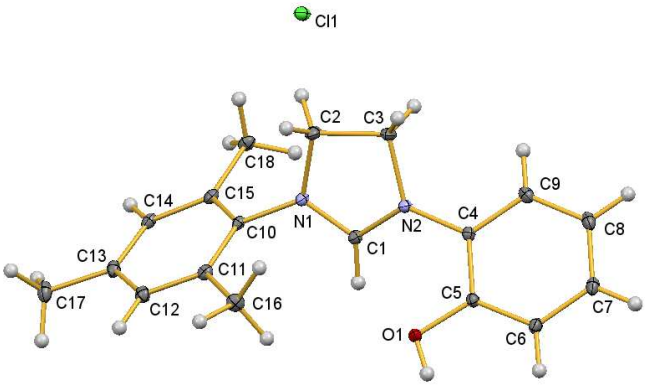

Figure S1. Crystal structure of 1-(2,4,6-trimethylphenyl)-3-(2-hydroxyphenyl)-4,5-dihydro-imidazolyl chloride salt **3c**.

Table S1. Crystal structure and refinement data for **3c**.

Compound	**3c**
Chemical formula	$C_{18}H_{21}ClN_2O$
Formula weight	316.82
Crystal size	0.341 x 0.231 x 0.070
Temperature/K	103(2)
Wavelength/Å	0.71073
Crystal system	Monoclinic
Space group	$P2_{1/c}$ (No.14)
a/ Å	12.3644(11)
b/ Å	8.8966(8)
c/ Å	14.9065(13)
α/ °	90
β/ °	94.3230(10)
γ / °	90
V/ Å^3	1635.1(3)
Z	4
ρ_{calcd}/ g cm^{-3}	1.287
Absorption coeff./ mm^{-1}	0.237
F(000)	672
Θ Range for data collection/ °	2.668 to 32.038
Reflections collected	25989
Independent reflections	5655 [R(int) = 0.0265]
Completeness to Θ/ %	98.6
Data/restraints/parameters	5655/0/206
Goodness-of-fit on F^2	1.080
Final R_1 indices [$I>2\sigma(I)$]	R1 = 0.0429, wR2 = 0.1135
R indices (all data)	R1 = 0.0459, wR2 = 0.1166
Largest diff. peak; hole/e Å^{-3}	0.676 and -0.201

Table S2. Selected bond lengths [Å] and angles [°] for **3c**.

O(1)-C(5)	1.3538(11)	C(13)-C(14)	1.3962(14)
O(1)-H(1O)	0.84(2)	C(13)-C(17)	1.5067(14)
N(1)-C(1)	1.3141(11)	C(14)-C(15)	1.3982(13)
N(1)-C(10)	1.4341(12)	C(15)-C(18)	1.5065(14)
N(1)-C(2)	1.4802(12)		
N(2)-C(1)	1.3204(11)	C(5)-O(1)-H(1O)	104.9(14)
N(2)-C(4)	1.4167(11)	C(1)-N(1)-C(10)	124.74(8)
N(2)-C(3)	1.4752(12)	C(1)-N(1)-C(2)	109.69(7)
C(1)-H(1)	0.9500	C(10)-N(1)-C(2)	124.06(7)
C(2)-C(3)	1.5346(14)	C(1)-N(2)-C(4)	125.99(8)
C(4)-C(9)	1.3931(13)	C(1)-N(2)-C(3)	109.43(8)
C(4)-C(5)	1.4069(13)	C(4)-N(2)-C(3)	123.93(8)
C(5)-C(6)	1.3980(12)	N(1)-C(1)-N(2)	113.48(8)
C(6)-C(7)	1.3921(14)	N(1)-C(1)-H(1)	123.3
C(7)-C(8)	1.3888(16)	N(2)-C(1)-H(1)	123.3
C(8)-C(9)	1.3937(14)	C(9)-C(4)-N(2)	120.11(8)
C(10)-C(11)	1.4028(13)	C(5)-C(4)-N(2)	119.50(8)
C(10)-C(15)	1.4048(12)	O(1)-C(5)-C(4)	117.94(8)
C(11)-C(12)	1.3946(13)	C(11)-C(10)-C(15)	122.16(8)
C(11)-C(16)	1.5065(13)	C(11)-C(10)-N(1)	118.79(8)
C(12)-C(13)	1.3974(14)	C(15)-C(10)-N(1)	119.05(8)

Symmetry transformations used to generate equivalent atoms:

Table S3. Torsion angles [°] for **3c**.

C(10)-N(1)-C(1)-N(2)	-169.84(8)	C(1)-N(2)-C(4)-C(9)	140.25(9)
C(2)-N(1)-C(1)-N(2)	-3.42(11)	C(3)-N(2)-C(4)-C(9)	-29.55(13)
C(4)-N(2)-C(1)-N(1)	-178.62(8)	C(1)-N(2)-C(4)-C(5)	-42.42(13)
C(3)-N(2)-C(1)-N(1)	-7.58(11)	C(3)-N(2)-C(4)-C(5)	147.78(9)
C(1)-N(1)-C(2)-C(3)	12.14(10)	C(9)-C(4)-C(5)-O(1)	179.52(8)
C(10)-N(1)-C(2)-C(3)	178.67(8)	N(2)-C(4)-C(5)-O(1)	2.20(12)
C(1)-N(2)-C(3)-C(2)	14.50(11)	N(2)-C(4)-C(5)-C(6)	-176.79(8)
C(4)-N(2)-C(3)-C(2)	-174.24(8)	C(1)-N(1)-C(10)-C(11)	59.35(12)
N(1)-C(2)-C(3)-N(2)	-15.27(10)	C(1)-N(1)-C(10)-C(15)	-120.65(10)

Symmetry transformations used to generate equivalent atoms: #1 -x+1,-y+1,-z+1

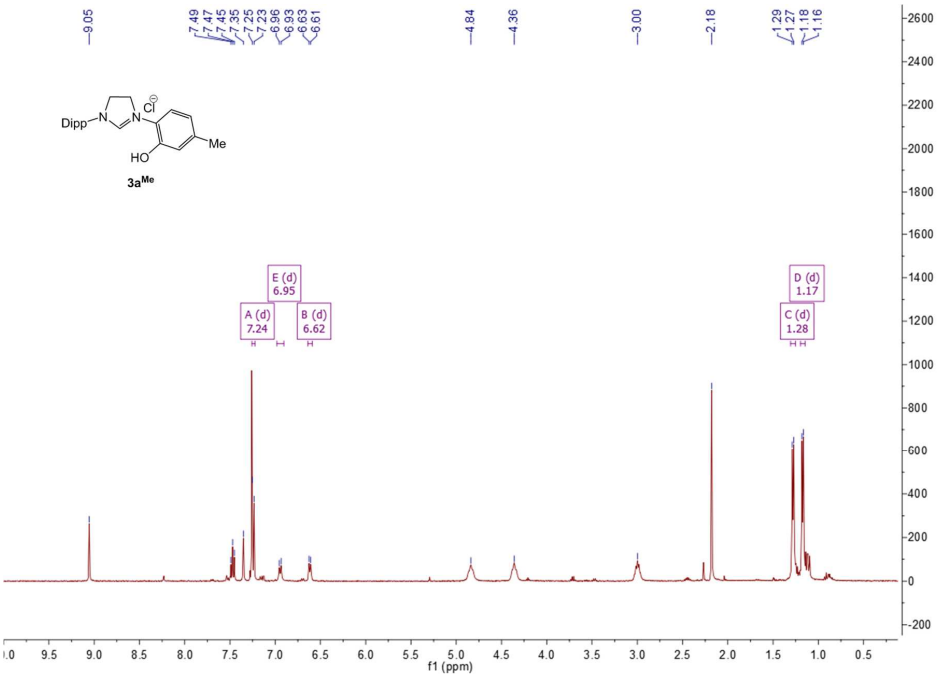

Figure S2. ^{1}H NMR spectrum of **3a^{Me}**.

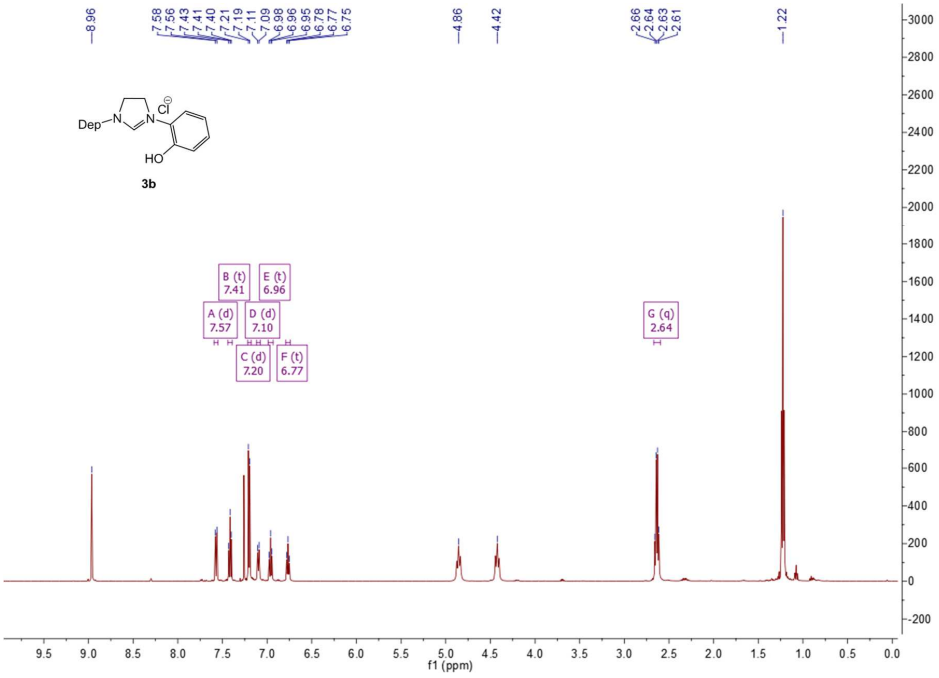

Figure S3. ^{1}H NMR spectrum of **3b**.

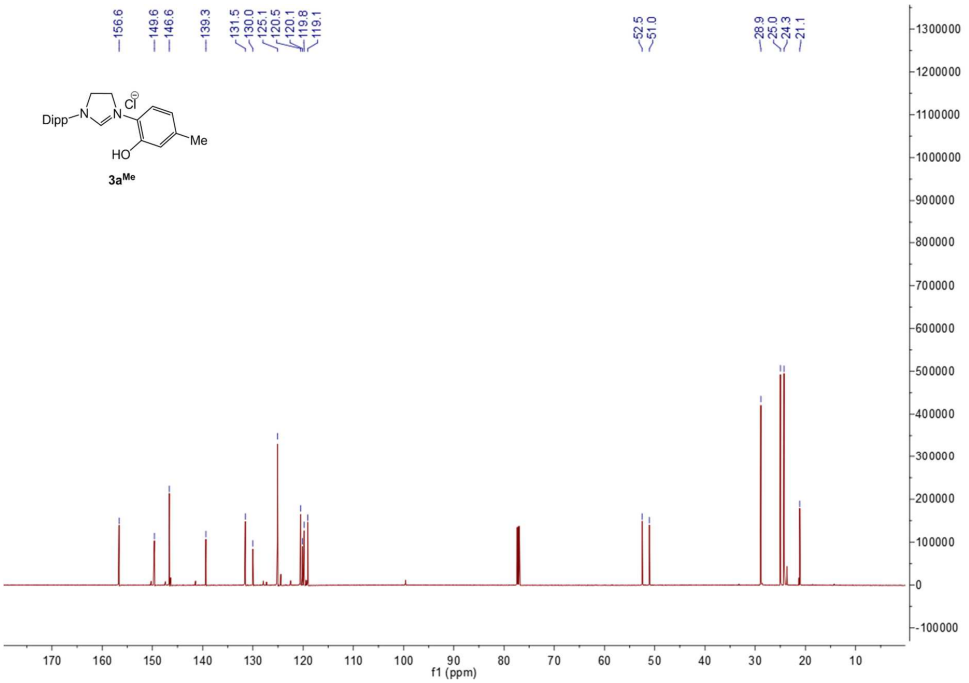

Figure S4. ^{13}C NMR spectrum of **3a^{Me}**.

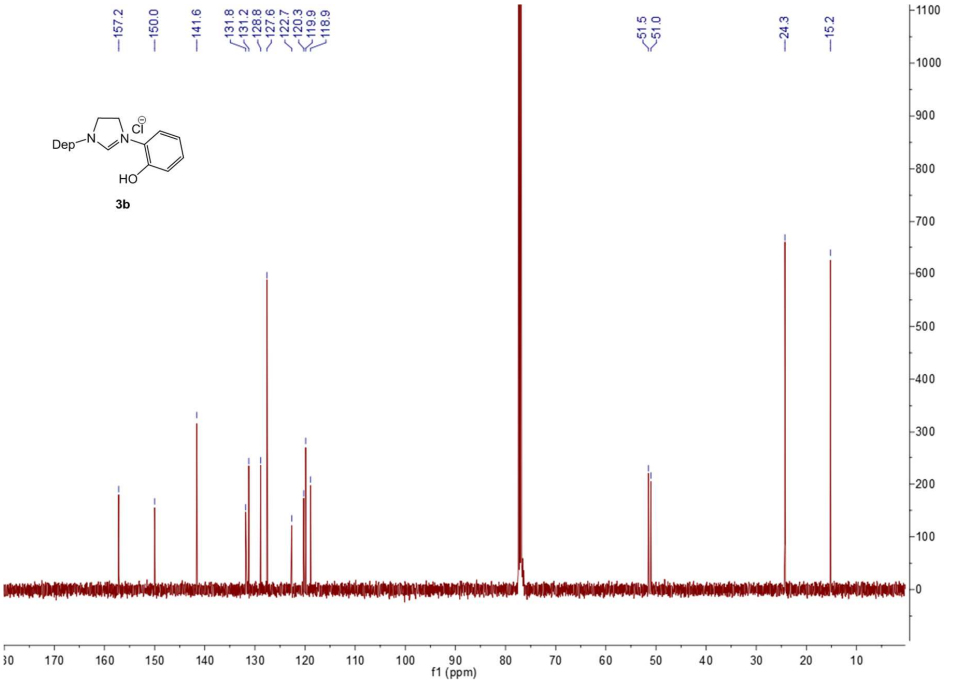

Figure S5. ^{13}C NMR spectrum of **3b**.

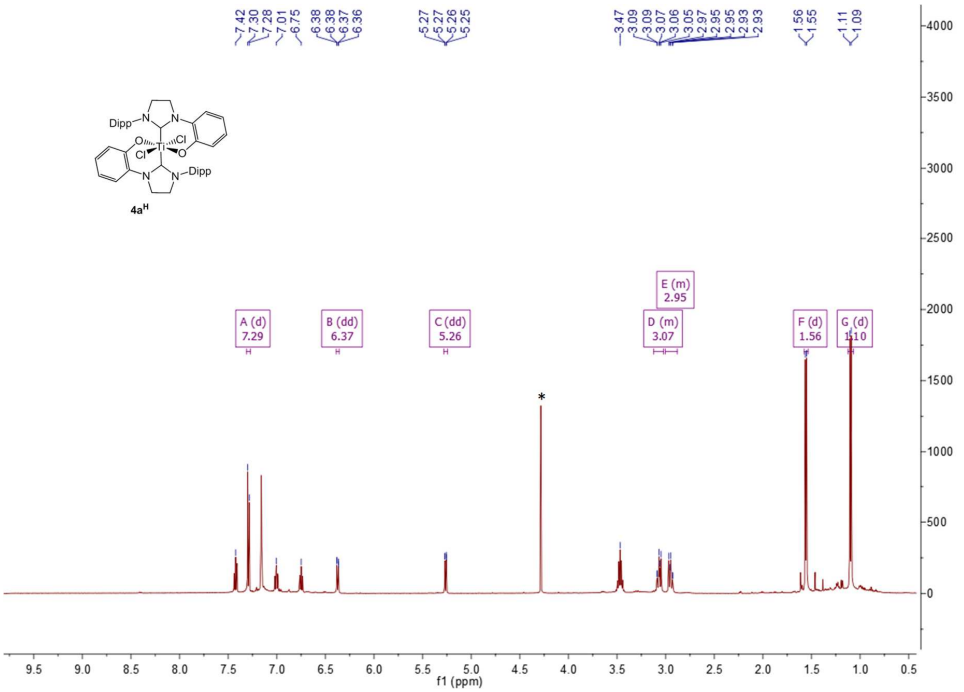

Figure S6. ^{1}H NMR spectrum of **4a^{H}**. (Residual solvent: * = CH_2Cl_2).

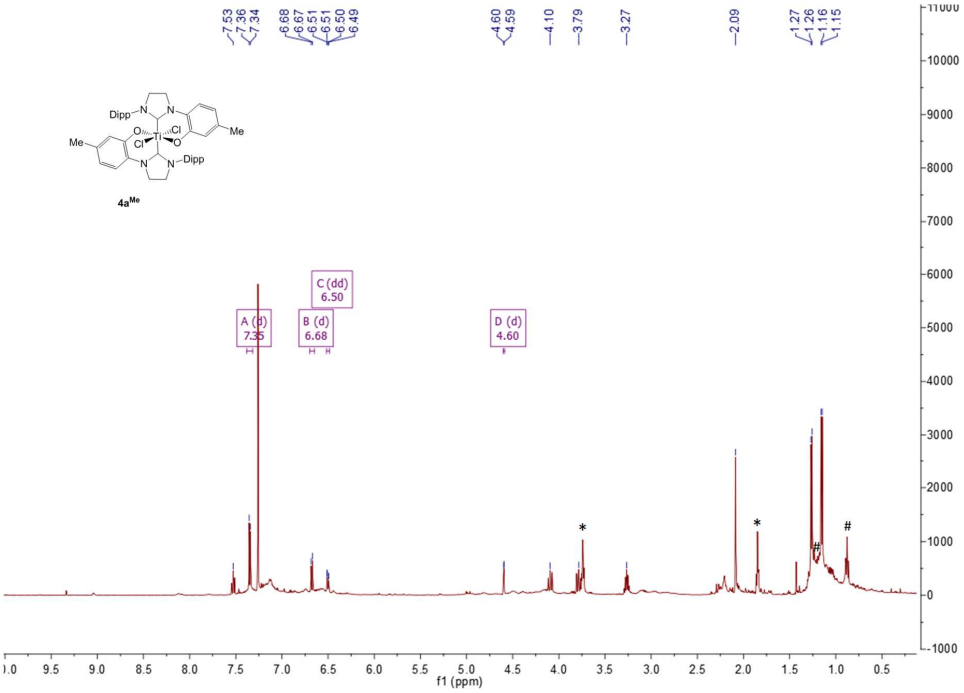

Figure S7. ^{1}H NMR spectrum of **4a^{Me}**. (Residual solvents: * = THF and # = hexane).

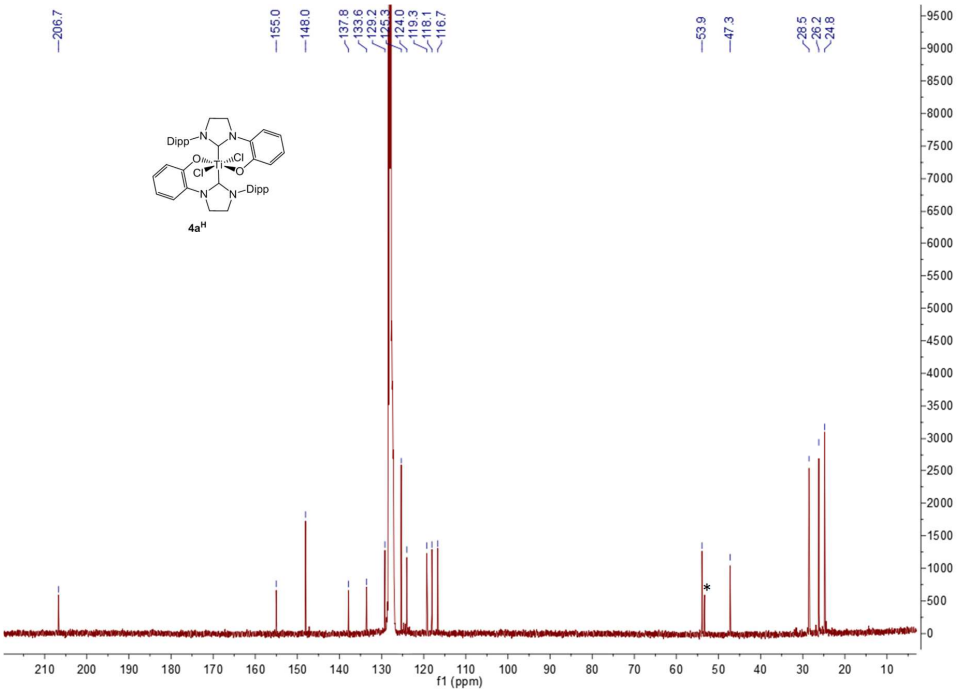

Figure S8. ^{13}C NMR spectrum of **4a^{H}**. (Residual solvent: * = CH_2Cl_2).

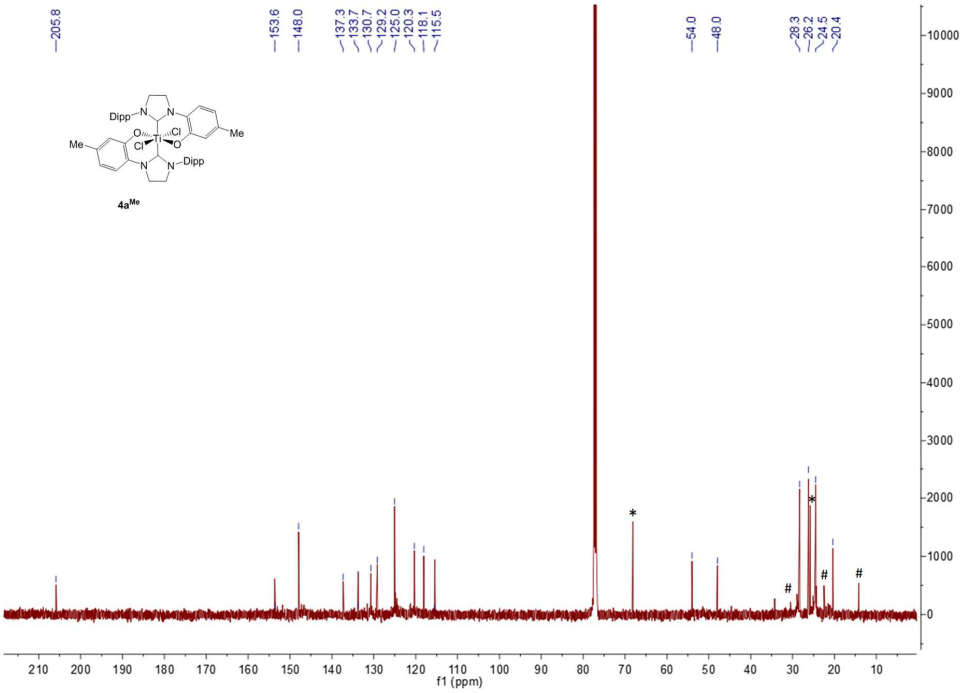

Figure S9. ^{13}C NMR spectrum of **4a^{Me}**.(Residual solvents: * = THF and # = hexane).

Table S4. Selected bond lengths [Å] and angles [°] for **4a^{H}**.

Ti(1)-O(1)#1	1.8578(12)	O(1)-Ti(1)-C(3)#1	97.60(6)
Ti(1)-O(1)	1.8579(12)	C(3)-Ti(1)-C(3)#1	180.00(8)
Ti(1)-C(3)	2.2597(18)	O(1)#1-Ti(1)-Cl(1)#1	89.29(4)
Ti(1)-C(3)#1	2.2597(18)	O(1)-Ti(1)-Cl(1)#1	90.71(4)
Ti(1)-Cl(1)#1	2.3269(5)	C(3)-Ti(1)-Cl(1)#1	95.27(4)
Ti(1)-Cl(1)	2.3269(5)	C(3)#1-Ti(1)-Cl(1)#1	84.73(4)
O(1)-C(1)	1.336(2)	O(1)#1-Ti(1)-Cl(1)	90.71(4)
N(1)-C(3)	1.353(2)	O(1)-Ti(1)-Cl(1)	89.29(4)
N(1)-C(2)	1.415(2)	C(3)-Ti(1)-Cl(1)	84.73(4)
N(1)-C(17)	1.480(2)	C(3)#1-Ti(1)-Cl(1)	95.27(4)
N(2)-C(3)	1.334(2)	Cl(1)#1-Ti(1)-Cl(1)	180.0
N(2)-C(4)	1.444(2)	C(1)-O(1)-Ti(1)	137.52(12)
N(2)-C(16)	1.476(2)	C(3)-N(1)-C(2)	128.42(15)
C(2)-C(1)	1.409(3)	C(1)-C(2)-N(1)	121.87(16)
		O(1)-C(1)-C(2)	119.94(16)
O(1)#1-Ti(1)-O(1)	180.0	N(2)-C(3)-N(1)	108.04(15)
O(1)#1-Ti(1)-C(3)	97.60(6)	N(2)-C(3)-Ti(1)	130.81(13)
O(1)-Ti(1)-C(3)	82.40(6)	N(1)-C(3)-Ti(1)	120.96(12)
O(1)#1-Ti(1)-C(3)#1	82.40(6)		

Symmetry transformations used to generate equivalent atoms: #1 -x+1,-y+1,-z+1

Table S5. Selected torsion angles [°] for **4a^{H}**.

C(3)-Ti(1)-O(1)-C(1)	36.52(18)	N(1)-C(2)-C(1)-O(1)	3.3(3)
C(3)#1-Ti(1)-O(1)-C(1)	-143.48(18)	N(1)-C(2)-C(1)-C(21)	-177.94(17)
Cl(1)#1-Ti(1)-O(1)-C(1)	131.74(17)	C(4)-N(2)-C(3)-N(1)	179.82(16)
Cl(1)-Ti(1)-O(1)-C(1)	-48.26(17)	C(4)-N(2)-C(3)-Ti(1)	-5.3(3)
C(3)-N(1)-C(2)-C(1)	9.9(3)	C(16)-N(2)-C(3)-Ti(1)	174.76(13)
C(17)-N(1)-C(2)-C(1)	-177.69(17)	C(2)-N(1)-C(3)-N(2)	176.37(16)
Ti(1)-O(1)-C(1)-C(2)	-36.0(3)	C(2)-N(1)-C(3)-Ti(1)	0.9(2)

Symmetry transformations used to generate equivalent atoms: #1 -x+1,-y+1,-z+1